Selective and Binary Adsorption of Anions onto Biochar and Modified Cellulose from Corn Stalks

Candelaria Tejada-Tovar [1],*, Ángel Villabona-Ortíz [1], Ángel Darío González-Delgado [2], Adriana Herrera-Barros [2] and Rodrigo Ortega-Toro [3]

[1]   Chemical Engineering Department, Process Design, and Biomass Utilization Research Group (IDAB), Universidad de Cartagena, Avenida del Consulado St. 30, Cartagena de Indias 130015, Colombia

[2]   Chemical Engineering Department, Nanomaterials and Computer-Aided Process Engineering Research Group (NIPAC), Universidad de Cartagena, Avenida del Consulado St. 30, Cartagena de Indias 130015, Colombia

[3]   Food Engineering Department, Food Packaging and Shelf-Life Research Group (FP&SL), Universidad de Cartagena, Avenida del Consulado St. 30, Cartagena de Indias 130015, Colombia

*   Correspondence: ctejadat@unicartagena.edu.co

Abstract: Water treatment alternatives such as adsorption using agricultural residues are currently being studied to eliminate pollutants that cause eutrophication in water bodies, avoiding the alteration of aquatic ecosystems. In this work, two bio-adsorbents were prepared using cellulose extracted from corn stems, *Zea mays*, which were labeled as *MC* (quaternized cellulose modified with Cetyl trimethyl ammonium chloride) and *B 1:1* (biochar obtained by the impregnation of the biomass with an H_2SO_4 solution, 50% *v/v*, using a ratio of 1:1% weight of biomass to volume, followed by carbonization at 520 °C for 30 min with a heating rate of 10 °C/min). FTIR, TGA, DSC, and SEM-EDS were used to study the properties of the bio-adsorbents. The effect of temperature over nitrate and phosphate adsorption in the selective and binary system at 100 mg/L was tested at five temperatures: 25, 30, 35, 40, and 45 °C, using a load of the pollutant of 100 mg/L, volume of 5 mL, and a rate of bio-adsorbent of 2 g/L at 200 rpm. Results showed a phosphate removal of 29.1% using the *B 1:1* bio-adsorbent at 30 °C and 23.8% with the *MC* bio-adsorbent at 35 °C. In the case of nitrate, removal of 40% was determined with the *B 1:1* bio-adsorbent at 25 °C, while removal of 38.5% was attained at 30 °C after using the *MC* bio-adsorbent. The equilibrium was reached at 420 min. Nitrate adsorption with the *MC* sample showed a good adjustment to the pseudo-second-order model. The pseudo-first-order model described the kinetics of phosphate removal with *MC*, while this model had a good fit with the *B 1:1* sample for nitrate and phosphate. Freundlich's model also adjusted the adsorption equilibrium for both anions with acceptable accuracy. Moreover, the binary study indicated selectivity for the phosphate, suggesting the potential applications of the carbon-based bio-adsorbents for anionic ions remotion in aqueous media.

Keywords: adsorption isotherms; bio-adsorption; biocarbon; kinetic equilibrium; quaternized cellulose

1. Introduction

Excessive plant growth on the surface of water bodies due to increasing nutrients such as nitrogen and phosphorus has become a problem worldwide, causing aquatic ecosystem degradation [1]. The pollution by nitrates and phosphates is highly interesting because they concur in both surface and groundwater [2]. Nitrogen and phosphorus are present in water bodies as nitrate (NO_3^-) and phosphate (PO_4^{3-}) anions. Due to anthropogenic activities, it has been an increase in the concentrations of these anions in the last decades, causing the deterioration of aquatic bodies and ecological systems. In addition, an overabundance of NO_3^- anions in water could produce childhood methemoglobinemia and many other types of cancers [3]. Phosphate is an anion highly soluble in water at standard temperature and pressure (25 °C and 100 kPa) [4]. Due to its high solubility, NO_3^-

has a smaller propensity for precipitation and adsorption; thus, an increase in temperature augments its solubility through exothermic reactions [5]. Moreover, NO_3^- and PO_4^{3-} have been frequently detected at concentrations ranging from 0.02 to 400 μM in the aquatic environment, threatening human health and ecosystems [6].

Several technologies have been implemented to mitigate the presence of NO_3^- and PO_4^{3-} in water, such as adsorption, bacterial assimilation, chemical precipitation, electrochemical methods [7], ion exchange [8], solid-phase denitrification, and reverse osmosis [9]. However, chemical and biological processes are limited by possible secondary contamination, strict reaction conditions [10], highly contaminated residues, and low efficiency at trace concentrations [11]. Bio-adsorption processes have significant potential as technology for wastewater treatment because they are characterized by using economical and highly available bio-adsorbents that can be prepared from agro-industrial wastes [12]. Many of the natural adsorbents used for anion removal include inorganic materials, e.g., MgAl nanocomposites supported on activated carbon [1], sepiolite [13], chitosan-supported hybrid bio-composites [14], nanoscale materials [15], and Mg–Al-modified biochar [16], among others, as well as biomasses from different sources, which have been used directly or chemically modified [10,11], obtaining good adsorption capabilities.

From elsewhere, bio-adsorption selectivity is the crypt to enhancing water treatment processes, considering the coexistence of pollutants in effluents and water bodies [17]. Research with multi-component scenarios is an advance in clarifying the complexity of the problem that needs to be considered when working with selective systems [17]. Producing adsorbents with high adsorption and selectivity capacity is essential to an ongoing investigation. Specific adsorbents remove have higher quantities of pollutants while are more selective at certain conditions [18]. Therefore, a rigorous analysis of adsorbents must be done to improve their performance and make them more efficient.

In this sense, post-harvest residues of agricultural and agro-industrial origins are desirable as adsorbents of contaminants in solution because they are abundant and inexpensive. Likewise, their lignocellulosic nature guarantees the presence of hydroxyl, carboxyl, phenol, methoxy, and other functional groups, which are determinants in the removal of cations [19]. However, the presence of these groups confers to the surface of lignocellulosic residues anionic properties suitable to retain metals. Still, electrostatic interactions would repel ions of anionic nature, as is the case of nitrates and phosphates [20]. Activated carbon from pine cones modified with lanthanum was evaluated for removing nitrate and phosphate, reaching an adsorption capacity of 68.2 mg/g and 46.6 mg/g using 0.1 g of adsorbent and 250 mg/L [21]. The rice, coconut, and coffee husk biochar were also used to remove the same nutrients, reaching adsorption capacities between 0.2 mg/g and 13 mg/g for nitrate and phosphate, respectively [22]. Similar results were obtained using brewer's spent grain quaternized with *N*,*N*-dimethylformamide, epichlorohydrin, [23] and sugarcane bagasse biochar modified with chitosan [24].

Therefore, cellulose-based adsorbents have been commonly modified to increase their capacity to retain substances of anionic origin and improve their selectivity. Quaternization is one of the most frequently used techniques to protonate the surface of adsorbents [25]. In this process, an etherification reaction is carried out by reacting a quaternary ammonium salt with the active centers at the cellulose structure, obtaining a positively charged adsorbent [26]. It has been used different nitrogen salts for the quaternization of bio-adsorbents, such as *N*,*N*-dimethylformamide [27], 2,3 Epoxypropyl trimethyl ammonium chloride [26], methyl trimethyl ammonium bromide [28], and epichlorohydrin [29]. In the present study, cetyltrimethylammonium chloride (CTAC) was chosen as a cellulose surface modifying agent; CTAC is a cationic surfactant with a quaternary ammonium head and a C16 alkyl tail [30]. Considering most of the previous studies, the methyl trimethyl ammonium bromide, a surfactant with a similar structure, was widely implemented in the surface modification of cellulose for use in the treatment of water contaminated with nitrate and phosphate.

This study focused on leveraging corn stalks as an adsorbent due to this agro-industrial residue's high availability on the Colombian Caribbean coast. Corn exploitation contributes widely to Colombia's agricultural production since it accounts for 13% of the national agricultural area. About 224,290 hectares are cultivated in the country, occupying the third place in the transitory crops, with about 1.8 million tons of production. The corn crop produces a large amount of biomass, of which about 50% is harvested as grain [31]. The rest corresponds to various plant structures, such as stalks, leaves, limbs, and cob. Of these residues, the stalks represent about 18% of corn's dry weight, equivalent to 16 to 25 tons per cultivated hectare [32].

In this study, corn stalks were used as a precursor for preparing two bio-adsorbents: one carbon type, modified with H_2SO_4 at a rate of 1:1% *w/v* (*B 1:1*), and cellulose extracted from biomass treated with cetyltrimethylammonium chloride (*MC*). Equilibrium and adsorption kinetics studies, structural characterization, and texture of the adsorbents were carried out. The literature has yet to report selectivity studies on nitrate and phosphate removal using cellulose extracted from *Zea mays* modified with CTAC. For this purpose, this work examines the selective and competitive adsorption of nitrate and phosphate on carbon-based bio-adsorbents (cellulose modified with CTAC and biochar) prepared from Colombian corn stalks; therefore, the present study contributes to the development of bio-adsorbents from agro-industrial wastes and their application for the remotion of anionic pollutants ions, as an eco-friendly solution to avoid the eutrophication in water bodies.

2. Materials and Methods

2.1. Materials and Reagents

Merck Millipore analytical grade reagents were used; monopotassium phosphate (KH_2PO_4) and sodium nitrate ($NaNO_3$) were utilized to prepare synthetic solutions at 100 mg/L. The pH was fixed with [1 M] of sodium hydroxide (NaOH) and hydrochloric acid (HCl) solutions. Cetyl trimethyl ammonium chloride (CTAC) at a concentration of 100 mM was used to modify the cellulose. At the same time, the chemical modification of the biochar was carried out using 99% analytic-grade sulfuric acid.

2.2. Synthesis and Characterization of the Bio-Adsorbents

The *Zea mays* corn stems were collected as agricultural waste from a local farm at Maria La Baja, Department of Bolivar, Colombia. The stalks were washed with deionized water and dried at 60 °C in an oven until regular mass. Subsequently, the biomass was reduced in size using an electric mill, selected by screening particles smaller than 0.14 mm for the extraction of cellulose and sizes between 1 and 2 mm for the preparation of the biochar.

For the extraction of cellulose, 20 g of the biomass of pulverized corn stalks were used, which were dispersed in distilled water with a ratio of 2% *w/v* using mechanical agitation at 200 rpm for 10 min; afterward, 500 mL of NaOH in solution at 4% *w/v* was added, continuing with agitation at 200 rpm for 2 h at 80 °C. Then, the solution was filtered, and the treatment with NaOH was repeated. Finally, the solution was filtered again, and the biomaterial was washed with abundant distilled water until the washing water was clear and with a neutral pH. The biomaterial obtained was dried at room temperature for 8 h and then added to a solution prepared by dissolving 50 g of Sodium chlorite ($NaClO_2^-$) in 500 mL of distilled water and 50 mL of sulfuric acid, stirring this mixture for 24 h at 30 °C. This experimental procedure obtained 6.2 g of cellulose, which was dried for 3 h at 60 °C [33]. For the chemical modification of the cellulose, it was added 62.8 mL of CTAC [100 mM] to 6.28 g of cellulose; the mixture was maintained with magnetic agitation for 24 h at 250 rpm at 27 °C [34]. The modified cellulose was rinsed with plenty of distilled water, dried at 50 °C, and stored in plastic vials.

The biochar was prepared by impregnating the biomass for 24 h with H_2SO_4 diluted at 50% *v/v*, using a chemical modification ratio of *1:1% w/v* (*B 1:1*). The carbonization was made in a muffle at 520 °C for 30 min, with a ramp speed heating function of 10 °C/min.

The biochar was washed with distilled water until neutral pH and dried at 100 °C until regular mass [17].

The morphology of the bio-adsorbents was analyzed by scanning electron microscope (SEM) coupled to energy dispersion spectrometry (EDS) using a scanning electron microscope TESCAN model FE-MEB LYRA 3, with gold coating, a voltage of 10 kV, and magnification of 1k×. The adsorbent total surface charge was determined through the point of zero charge pH (pH_{pzc}) [35]. For this, 0.5 g of adsorbent was put in contact with 50 mL of deionized water at different pH values from 2–11 for 24 h at room temperature; then, the final pH of the solution was measured, and the results were plotted, establishing that the pH_{PZC} is the value where the initial pH slope intersects with the final pH curve.

2.3. Selective Adsorption Experiments

Adsorption tests were developed using an experimental design, which considered as response variables the removal efficiency (R) of phosphate and nitrate anions; the effect of the temperature was evaluated at five levels: 25, 30, 35, 40, and 45 °C. The concentration of the contaminants after bio-adsorption was measured in a spectrophotometer model BK-UV1900 brand Biobase UV-VIS.

Synthetic solutions were prepared at 100 mg/L, using the following protocol: 0.439 g of dehydrated KH_2PO_4 was added to 1 L of distilled water to prepare the phosphate solution [36]; for the nitrate solution, KNO_3 was dried in an oven at 103–105 °C for 24 h, followed by the addition of 0.7218 g was dissolved in 1 L of deionized water, and 2 mL of chloroform was added to preserve the solution [37]. Adsorption experiments were performed by contacting 5 mL of synthetic contaminant solution with doses of bio-adsorbents of 2 g/L, using an orbital agitator at 200 rpm, varying the temperature in the range selected for this study.

The remaining concentrations of contaminants (C_e) were determined by UV-Vis spectroscopy: phosphate concentration detection was performed at 880 nm following the ascorbic acid method with a limit of detection (LOD) of 0.03 mg/L [36], and nitrates were determined at 543 nm (LOD 0.05 mg/L) [37]. A correction was made to rule out the possible presence of nitrites by performing a second measurement at 275 nm (LOD 0.01 mg/L). The correction was made for all the nitrate samples to determine the possible presence of nitrites. The removal efficiency (R) was determined according to Equation (1):

$$R(\%) = \frac{C_0 - C_e}{C_0} \times 100 \tag{1}$$

where C_0 and C_e are the feed and final concentrations of anions in the solution, both expressed in mg/L.

2.4. Adsorption Isotherms

Equilibrium experiments were conducted using five different levels of concentrations of the anions from 20–100 mg/L for 24 h, using a volume of 100 mL and 2 g/L of adsorbent. The Langmuir (Equation (2)) and Freundlich (Equation (3)) models were applied to adjust the experimental data obtained at equilibrium time. The Langmuir model is a process where the adsorbate creates a single layer on the surface of the adsorbent until the balance between liquid and solid is achieved [38]; it also considers that the exposed area of the adsorbent is homogeneous which possesses a certain quantity of available sites that have equal energy capable of adsorbing a single species.

$$q_e = \frac{q_{max}K_L C_e}{1 + K_L C_e} \tag{2}$$

C_e is the anions final concentration (mg/L), q_e is the quantity of pollutant adsorbed per gram of adsorbent at equilibrium (mg/g), q_{max} is the maximum capacity in the single layer, and K_L is Langmuir's isothermal constant.

Freundlich's isotherm deduces that the adsorption process occurs in multiple layers from the exposed surface into the pores of the adsorbent [20].

$$q_e = K_F C_e^{1/n} \tag{3}$$

where q_e (mg/g) is the final adsorption capacity of adsorbent, K_F (L/g) is Freundlich's isothermal constant, and C_e (mg/L) is the concentration of adsorbate at equilibrium.

Other isotherm models, such as Temkin's [39], were tested, but given the fit value obtained, it was decided not to report it to reduce noise in the graphs and tables.

2.5. Adsorption Kinetics

Adsorption kinetics experiments were conducted at the best temperature condition found in experiments, at 100 mg/L using 100 mL of solution volume and 2 g/L of adsorbent load [40], 200 rpm of stirring rate and sampling in 5, 10, 20, 30, 60, 180, 300, 420, and 1440 min for each experiment. The pseudo-first-order (Equation (4)), pseudo-second-order (Equation (5)), and Elovich (Equation (4)) models were adjusted to analyze the experimental kinetic data. The pseudo-first-order Lagergren model assumes that the reaction rate is controlled by only one of the reagents [41].

$$q_t = q_e \times \left(1 + e^{-k_1 t}\right) \tag{4}$$

where k_1 (min^{-1}) is the time scale factor whose value determines how quickly equilibrium can be reached in the system, q_e, and q_t (mg/g) are the quantities adsorbed per unit of mass at equilibrium at any time t, respectively.

The pseudo-second-order equation contemplates that the process limit step is chemisorption, which occurs by ion exchange produced at the surface of the adsorbent. The reaction order is two regarding the number of adsorption sites available for exchange [42].

$$q_t = \frac{t}{\frac{1}{k_2 \times q_e^2} + \frac{t}{q_e}} \tag{5}$$

where α is the initial adsorption rate (mg/g min), β (g/m^{-1}) is the desorption constant, and q_t (mg/g) is the amount of retained pollutant in a time t.

2.6. Adsorption Multi-Component System

The multi-component adsorption experiments were conducted by placing 150 mL of equimolar contaminant solution with an adsorbent dose of 2 g/L in contact for 24 h. The solution was prepared by mixing 50 mL of each solution (nitrate or phosphate) at 100 mg/L. The separation was made using microfilters of 0.45 µm. The sample for nitrate analysis was stored in plastic vials, while the sample for phosphate examination was stored in amber glass vials and subsequently refrigerated until analysis.

3. Results and Discussion

3.1. Characterization of the Bioadsorbents

Figure 1 shows the thermal stability analysis by determining the weight change of the synthesized cellulose over 0–100 °C (TGA) and the heat flow of a sample at the same temperature range (DSC). These analyses showed that the cellulose extracted from corn stalks exhibits three stages of weight loss. First, a weight loss of 10% at the temperature range from 30–225 °C can be attributed to the evaporation of water and adsorbed humidity due to the hydrophilic character of the lignocellulosic materials [43]. Additionally, a second weight loss of 70% was determined between 250–400 °C; this primary loss and its gradual thermal transitions are related to the cellulosic chain degradation [44] through the decomposition of glycosyl units followed by its transformation to char [45], as well as hemicellulose and a small quantity of cellulose [43]. The last weight loss observed from

400–600 °C was 21%, characteristic of the lignin decomposition. These results confirmed the purity of the extracted cellulose from corn stalks.
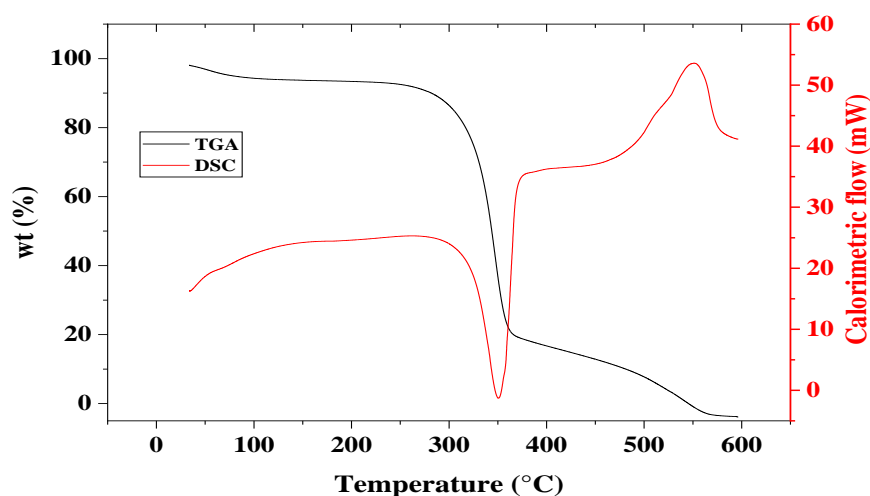

Figure 1. Thermal stability analysis of the cellulose extracted from the corn stalks.

Figure 2 shows the FTIR spectra for CTAC-modified corn stalk cellulose previously and afterward of the adsorption of nitrate and phosphate.
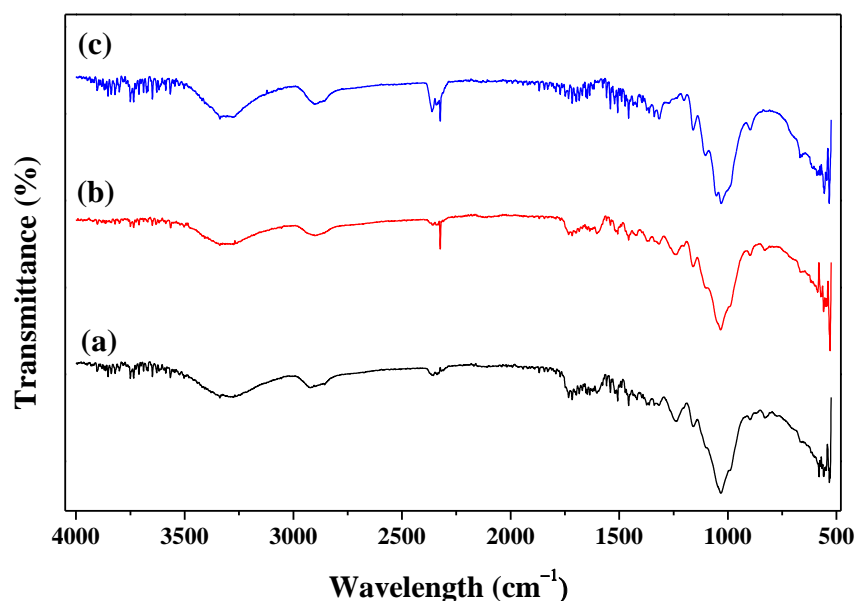

Figure 2. FTIR spectra of MC before and after adsorption of nitrate and phosphate for (**a**) MC, (**b**) MC-Nitrate, and (**c**) MC-Phosphate.

According to Figure 2, the three spectra were similar to a sharp and broad peak at 3350 cm^{-1}, caused by the stretching vibration of the OH group and tertiary amines; thus, due to the vibration of the groups in cellulose and hemicellulose, as can be seen from the FTIR of cellulose from the literature [46]. The appearance of amines and carbonyls by the stretching vibrations of the O-H tie is located between 3400 and 3500 cm^{-1} [21,22]. The peak caused by C-H presence is observed at 2904 cm^{-1}. Wavelengths between 2000 and 2500 cm^{-1} show weak C≡C and COOH^{-} signals. The typical band assigned to cellulose is observed in the region between 1669 and 829 cm^{-1}, with stretching and bending vibrations due to -CH$_2$ and -CH, -OH, and C-O bonds in the cellulose bonds [47]. The crystalline structure of cellulose is reflected around 1418 cm^{-1}, while around 900 cm^{-1} is related to its amorphous form [34]. The intense peaks at 1130 cm^{-1} in MC can be associated with

the specific stretching vibration of the C-N bond, corresponding to the surface modification of the material with the quaternary amino group of CTAC [48]. The peak around 850–550 cm^{-1} is attributed to the stretch of the C-Cl group, caused by the union of the chloride to the alkyl group of modified cellulosic material; also, the CTAC was identified at bands at 2892 cm^{-1} and 2921 cm^{-1} consistent with symmetrical and asymmetrical CH$_2$ stretches from the long alkyl CTAC chain, accordingly with Hastati et al. [49]. In the MC spectra, a peak near 1480 cm^{-1} is characteristic of the trimethyl groups of the quaternary ammonium [49]. After adsorption, it is evident that bands are widening from 1050 cm^{-1} to 1650 cm^{-1} due to phosphate removal [50]. The characteristic nitrate peak at 1380 cm^{-1} indicates its retention by MC [51]. FTIR results prove the existence of active centers and demonstrate that MC could remove the anions under study present in the aqueous phase by the union in the region where the peaks of the modifying agent were found.

The morphology of the bio-adsorbent synthesized from corn stalks was studied by SEM analysis coupled with EDS (Figure 3). The chemically modified cellulose (MC) shows a slightly porous surface with multiple folds and tubes, which is attributed to the delignification of the raw material (Figure 3a) [52]. Similar results were reported by Eleryan et al. [53], revealing that the particle surface contains wide pores, which are available for ion adsorption within the surface pore. The biochar modified with H$_2$SO$_4$ exhibited a heterogeneous surface of porous nature in the range of macro and mesopores, allowing access to the microporous structure (Figure 3b) [54]. In addition, agglutinated networks were observed due to the volatilization of oxygen and hydrogen present in lignocellulosic compounds of low aromaticity and the lignin material, causing the carbon to form new aromatic links, increasing the order of graphitization in the structure [55]. Previously, it was found that NO$_3^-$ and PO$_4^{3-}$ removal was enhanced due to surface modification with Al of biochar synthesized from poplar residues [56]. The bromatological composition of corn stalks has been reported, which presents in their structure cellulose (35–50%), hemicelluloses (20–35%), and lignin (15–20%); the quaternization of the structure could be successful when occurred between hydroxyl groups of these lignocellulosic materials [57].
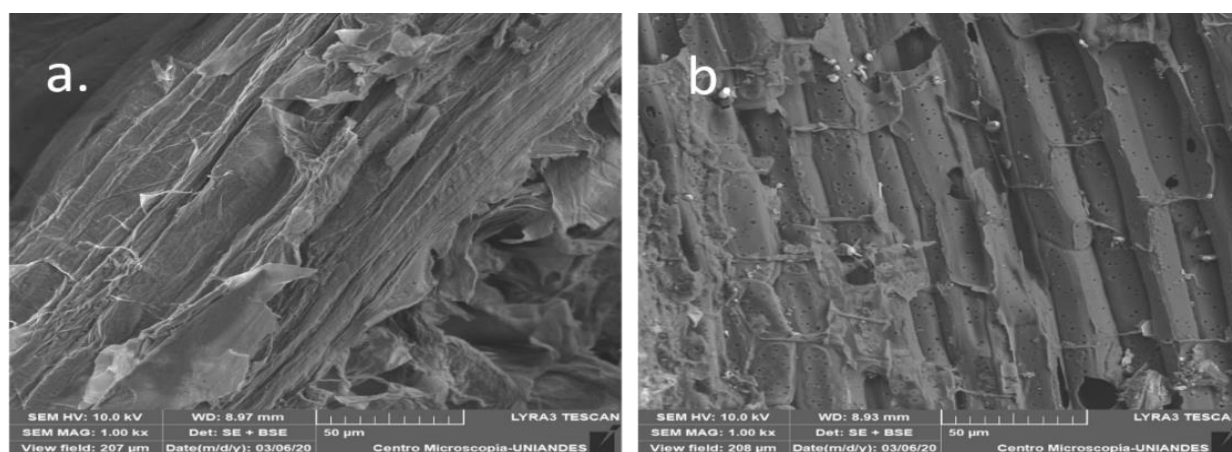

Figure 3. SEM micrographs of (**a**) the chemically modified cellulose (MC) and (**b**) the biochar prepared by impregnation with H$_2$SO$_4$ B 1:1.

From the EDS images, C, O, S, and K atoms were observed in higher proportions. The presence of sulfur in the structure of B 1:1 is related to the chemical modification with H$_2$SO$_4$ evidencing the success of the process. The MC sample did not display any change in its structure after the modification with the chemical reagent CTAC. Table 1 shows a compilation of the elemental composition measured by EDS.

From the data presented in Table 1, it was observed that the MC sample did not report the presence of Mg and Si atoms, nor P, S, and K atoms; this can be attributed to the purification of the cellulose with NaClO$_2^-$, which was used for the bleaching and removing of lignin and pectin traces from the biomass [33]. Meanwhile, in the biocarbon beyond the

presence of S atoms in high proportion, it was found the presence of elements, such as Mg, Si, P, S, and K; the above, considering that the B 1:1 sample was synthesized from corn stalks without any pre-treatment and those elements are present in the raw fiber surface in trace amounts [58].

Table 1. Bio-adsorbent elementary composition determined from the EDS technique.

Element	% Weight	
	MC	B 1:1
C	52.14	80.26
O	47.69	9.43
Al	0.140	0.00
Mg		0.32
Si		0.70
P		0.30
S		7.16
K		1.84

The pH value of the liquid phase is an essential component impacting anion adsorption on bio-adsorbents; this variable significantly affects the exchange capacity between the active centers and the adsorbent materials [59]. NH_4^+ is the main form of NH_3 in a weakly acidic or neutral solution, and an ionic swap will happen between NH_4^+ and species charged positively on the adsorbent. Nevertheless, a significant part of the NH_4^+ is transformed into NH_3 under pH > 7; the adsorbent cannot capture the anionic pollutant [10]. The increase in ammonium adsorption capacity on biochar has been reported with the pH variation from 4 to 8, decreasing this value in alkaline media [59]. The lower ammonium adsorption when pH is less than four can be attributed to the competence between hydronium and NH_4^+ for the adsorption sites on the exposed surface of the materials. In addition, the effect of this variable is also essential for phosphate adsorption since the adsorption process occurs between the positively charged bio-adsorbent and the negatively charged PO_4^{3-} [59]. Thus, nitrate and phosphate are scarcely adsorbed under alkaline conditions because OH⁻ ions compete with nitrate ions for available adsorption sites [13]. The pH_{pzc} was determined to establish the pH at which the surface load of the bio-adsorbents is zero [60]. It was found that the pH_{PZC} was 6.06 and 5.17 for modified cellulose (MC) and biochar (B 1:1), respectively. The raw biomass exhibited a pH_{PZC} of 7.14, and the value for the cellulose was 4. The increase in the pH_{PZC} of the MC was reported for crosslinked cellulose-epichlorohydrin. It was attributed to the quaternization of the biomass [61] and the modification done in the present study. Elsewhere, the zeta potential of cellulose at pH 4 has been reported to be zero, which is consistent with the results obtained in the present study for the cellulose extracted from corn stalks [62]. At a pH lower than pH_{PZC}, the bio-adsorbents behave as a positively charged structure, while as the pH of the solution augments, a de-protonation of their surface occurs [9]. Thus, it was established that the pH value at which the adsorption tests were performed using the two bio-adsorbents was 4 to ensure the positive charge of the biomaterial's surface.

3.2. Effect of Temperature

Adsorption tests were performed at pH 4, evaluating the change in temperature between 25 and 45 °C. Figure 4 shows the results of removal capacity. It was found that the best phosphate removal efficiencies were observed at 30 °C using the B 1:1 sample, reaching an efficiency of 29.1%, and at 35 °C using the MC sample, obtaining a value of 23.8%. In nitrate, the effect of temperature was more noticeable, observing a removal efficiency of 40% using the B 1:1 bio-adsorbent at 25 °C and 38.5% with the MC bio-adsorbent at 30 °C. Therefore, it can be said that the process does not need an energy supply to happen by the exothermic nature of reactions [63]. The modified cellulose exhibited selectivity for the phosphate anion, while the biochar showed selectivity for the nitrate. However,

the removal efficiencies of the two adsorbents were low in comparison to information reported in the literature for adsorbents of different natures (quaternized resin grafted with chitosan [64] and quaternized Chinese cane [25]). When using a nano adsorbent functionalized with zerovalent iron, 16% and 63% removal efficiencies were reported at pH 11 and 3, respectively [59]. The evaluation of various adsorbents showed that pH did not significantly affect the nitrate removal efficiency when using mineral and HCl-activated sepiolite [13]. The increase in nitrate and phosphate removal efficiency with increasing temperature when using adsorbents functionalized with amino groups demonstrates the endothermic character of the anion removal process [65]. In addition, the diminution of process yield when temperature increases is caused by solubility; rising temperature increases the solubility of anions of exothermic nature, improving the adsorbent's ability to retain ions in its structure because temperature acts as a driving force for adsorption processes [5].
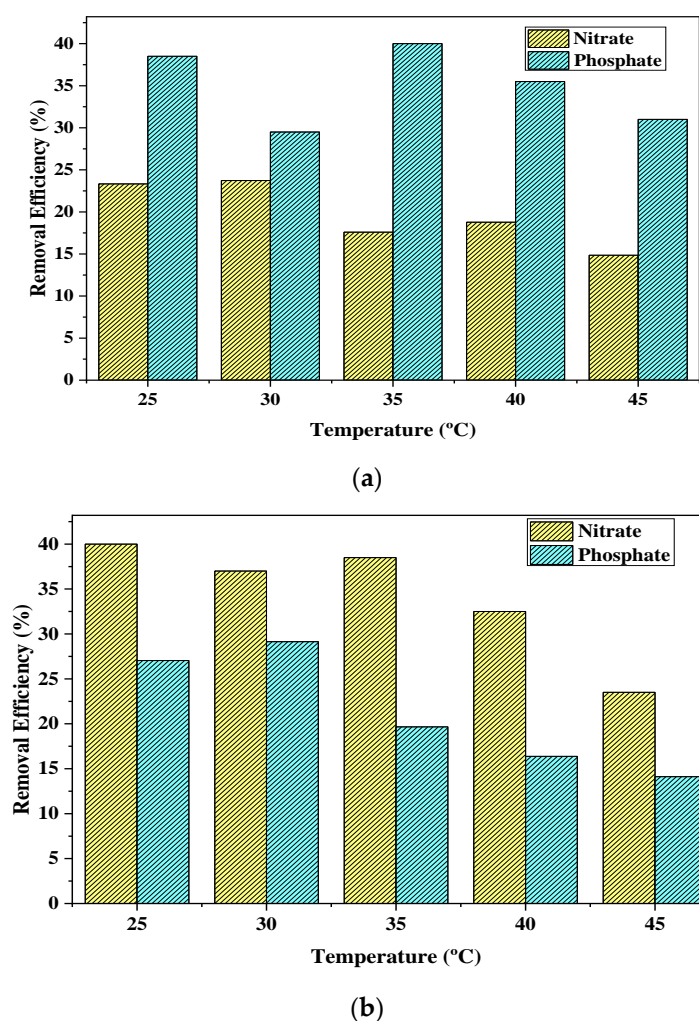

(**a**)

(**b**)

Figure 4. Nitrate and phosphate removal efficiency using bio-adsorbents prepared from corn stalks (**a**) modified cellulose (MC) with the chemical agent CTAC; and (**b**) biochar impregnated with sulfuric acid (B 1:1).

The behavior of the adsorbents regarding the pollutants are related to their elementary composition (Table 1) and their folded and tubular morphology (Figure 3). Thus, it has been reported that the removal of nitrate and phosphate onto bio-adsorbents modified with quaternary amine groups could have happened by several possible mechanisms, in which electrostatic pull, ion exchange, and formation of surface complexes are implicated due to the heterogeneity of their structure and binding sites [9].

3.3. Adsorption Equilibrium

Adsorption equilibrium was studied by determining the isotherms at the best experimental temperature conditions found (30 °C for nitrate and phosphate with MC and phosphate with B 1:1, and 25 °C for nitrate with B 1:1). It varied the initial concentration of contaminants in 20, 40, 60, 80, and 100 mg/L, 200 rpm, using 2 g/L of adsorbent. Figures 5 and 6 show the experimental data adjustment to Langmuir and Freundlich's models, employing non-linear regression with the OriginPro 8® software. The adjustment parameters are displayed in Table 3. The best fit was selected according to the R^2 value [66].
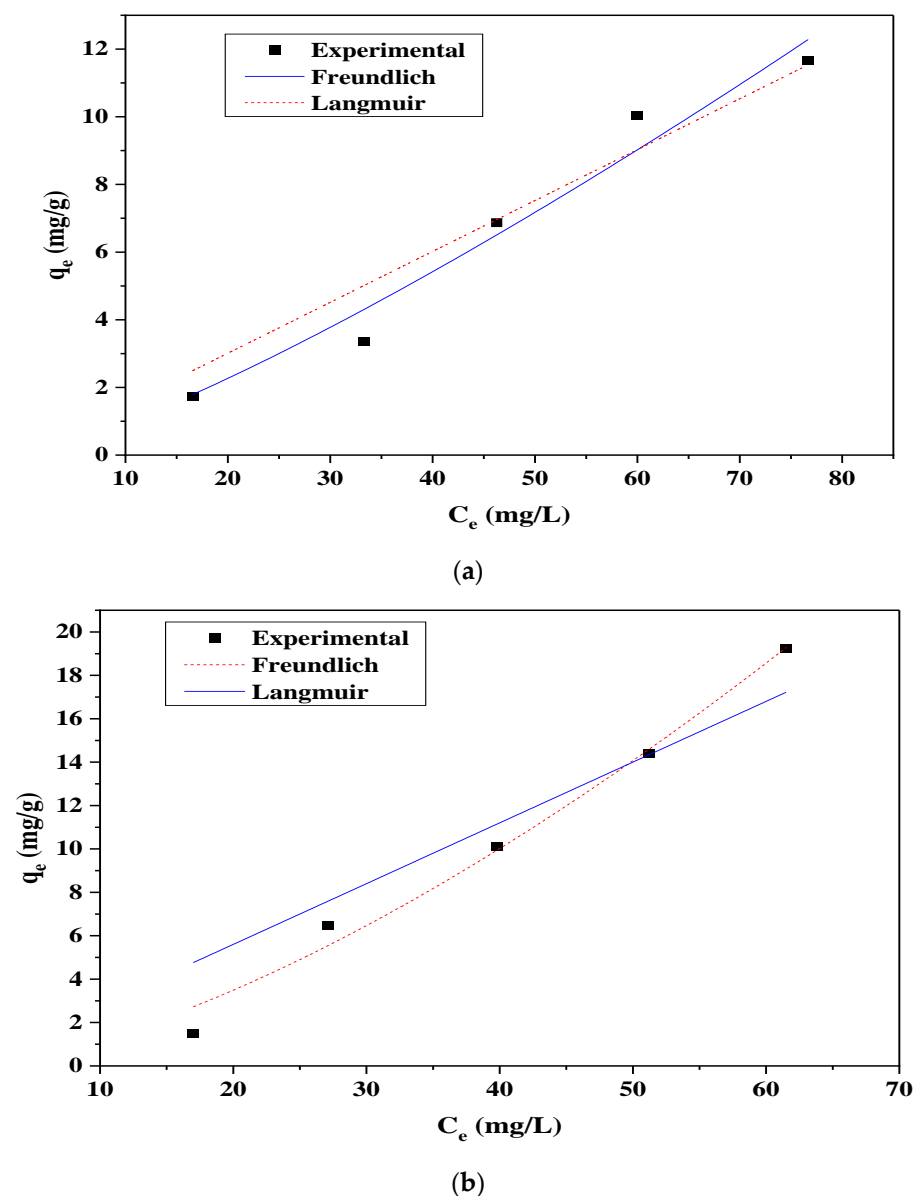

(a)

(b)

Figure 5. Fit to isothermal non-linear models of adsorption equilibrium experimental data of (**a**) nitrate and (**b**) phosphate using modified cellulose (MC) as adsorbent.

Langmuir coefficients for the linearized equation were obtained by making graphs between C_e/q_e versus C_e. Freundlich coefficients for the linearized Freundlich equation were obtained by building graphs between log (q_e) versus log (C_e). The calculated parameters are shown in Table 2. It can be inferred that linear Langmuir equations show different constants against non-linear adjustment, as error variation indicates (comparing results from Tables 2 and 3).
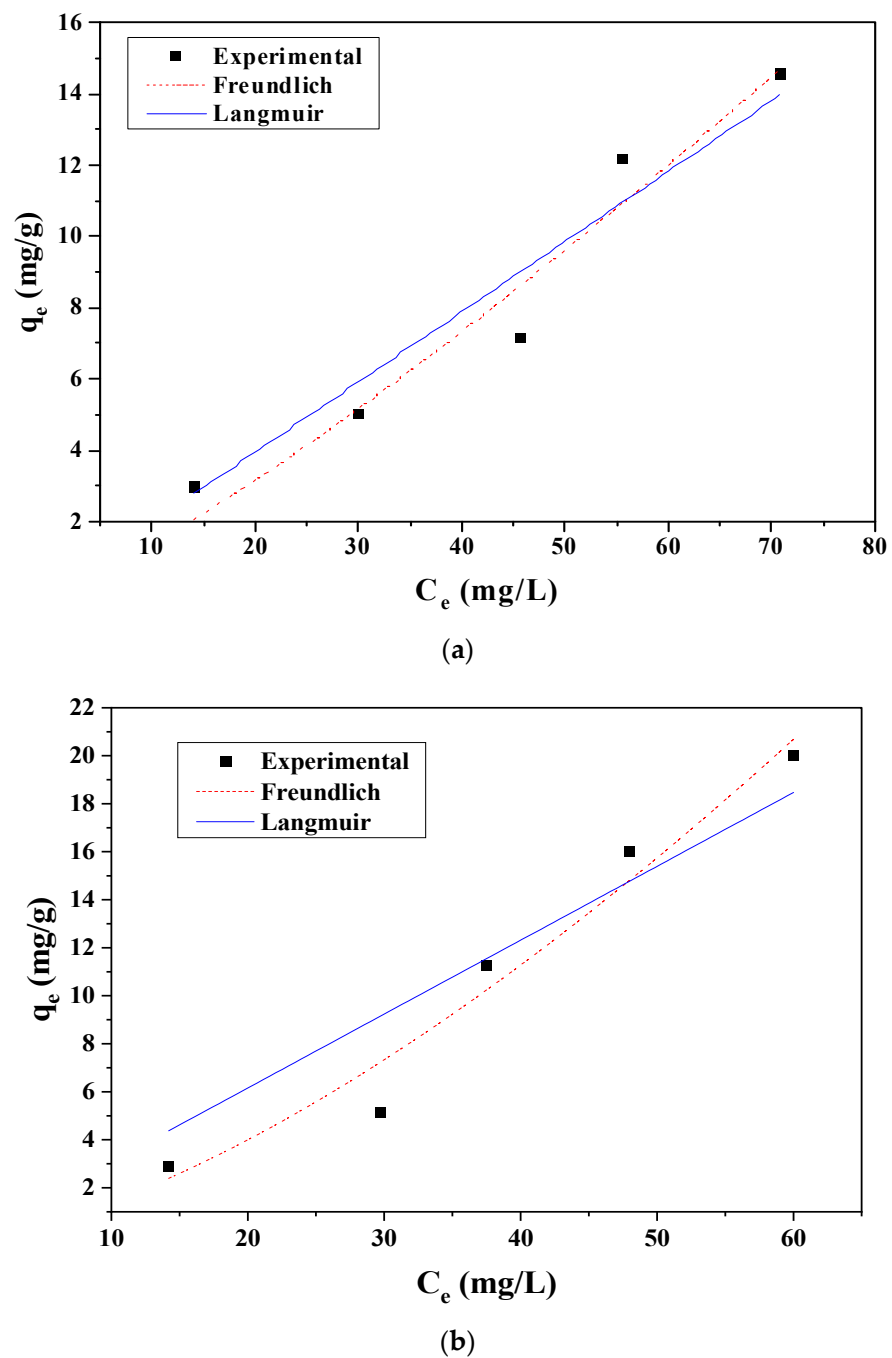
(**a**)

(**b**)

Figure 6. Fit to isothermal non-linear models of the adsorption equilibrium experimental data of (**a**) nitrate and (**b**) phosphate using biochar (B 1:1) as adsorbent.

Table 2. Adjustment parameters of NO_3^- and PO_4^{3-} non-linear adsorption isotherms.

	Freundlich			Langmuir		
	K_f	n	R^2	q_{max} (mg/g)	K_L (L/mg)	R^2
MC-N	0.0526	0.7957	0.9546	331.6291	7.32×10^{-6}	0.9196
MC-P	0.0366	0.6573	0.9832	586.4403	5.03×10^{-6}	0.8792
B 1:1-N	0.082	0.822	0.937	161.0802	8.81×10^{-6}	0.914
B 1:1-P	0.0452	0.668	0.952	586.0917	5.53×10^{-6}	0.857

Table 3. Adjustment parameters of NO_3^- and PO_4^{3-} adsorption linearized isotherms models.

	Freundlich			Langmuir		
	K_f	n	R^2	q_{max} (mg/g)	K_L (L/mg)	R^2
MC-N	0.039	0.755	0.974	1.461	15.276	6.07×10^{-3}
MC-P	0.009	0.528	0.952	9.059	6.779	1.33×10^{-2}
B 1:1-N	0.190	1.001	0.947	0.726	163.934	1.093×10^{-3}
B 1:1-P	0.520	3.299	0.996	9.158	18.018	9.091×10^{-3}

Note: RMSE: absolute error measure.

From the data summarized in Tables 2 and 3 and the adjustments in Figures 5 and 6, it was established that Freundlich was the model that best describes the adsorption of nitrate and phosphate, with $R^2 > 0.90$ in all cases. Although the adjustment is not ideal, the accuracy is fair compared with other models evaluated as Temkin. The above indicates that the anion adsorption process happens in multilayers due to the heterogeneous surface of the bio-adsorbents prepared from corn stalks [67]. The value of n was <1 in all cases, indicating low favorability of the process over bio-adsorbents [68]. It has been reported previously, also exemplifying the Freundlich model, for removing nitrate that activated carbon modified displayed a high affinity between the bio-adsorbent and the contaminant [34]. When using halloysite and kaolinite functionalized with triethanolamine in the elimination of NO_3^- and PO_4^{3-}, an adjustment of the isotherm to the Freundlich model with R^2 higher than 0.85 were reported in all cases, and a high affinity between the active centers of the adsorbents and the contaminants [69]. As Donnan's theory illustrates [70], anion charge is an essential feature of the yield in the adsorption mechanism; it may lead to selective phosphate adsorption on both adsorbents evaluated against nitrate. Thus, considering that the adsorption of both anions under study has been reported to occur by Van der Waals forces, ion exchange and surface complex formation are involved due to the heterogeneity of their structure and binding sites [8,57].

3.4. Adsorption Kinetics

The effect of contact time was evaluated by determining kinetics. Elovich's pseudo-first and pseudo-second-order models adjusted the obtained data and identified possible mechanisms during adsorption [48]. The adsorption kinetics are presented in Figure 6, and the models' adjustment parameters are shown in Table 4.

Table 4. Kinetic Model Adjustment Parameters.

Model	Parameter	MC		B 1:1	
		Nitrate	Phosphate	Nitrate	Phosphate
Pseudo-first order	k_1 (min^{-1})	0.0147	0.0073	0.021	0.010
	q_e (mg/g)	11.2036	19.6829	14.398	20.137
	R^2	0.9741	0.9867	0.989	0.985
Pseudo-second order	k_2 (g/mg × min)	0.0014	3.60×10^{-4}	0.0016	5.04×10^{-4}
	q_e (mg/g)	12.5699	22.9392	15.849	23.237
	R^2	0.9827	0.9629	0.981	0.956
Elovich	α (mg/g × min)	0.6375	0.5361	1.113	0.704
	β (g/mg)	0.4523	0.2392	0.366	0.222
	R^2	0.9430	0.9013	0.905	0.894

The q_{max} was obtained with sample B 1:1 (Figure 7), reaching the adsorption equilibrium at about 420 min in all cases, with a fast removal rate during the first minutes because

of the high quantity of vacant adsorption sites in the biocarbon at the beginning of the process [71]. Nitrate adsorption using the MC sample showed a good fit to the pseudo-second-order model, so it is established that the rate-limiting step is a chemical reaction due to the physicochemical interactions between the two phases [14]. The pseudo-first-order model described the kinetics of phosphate removal with the MC bio-adsorbent and nitrate and phosphate on the B 1:1 bio-adsorbent, thus establishing that the adsorption rate happens at an active site at the time [48]. The fit of both models suggests a chemical mechanism, and the rate of remotion is controlled by electrostatic forces between the anions and the bio-adsorbent [46]. Also, the adjustment to pseudo-first-order meant that the external mass transfer process was more effective in controlling the mercury adsorption process of coffee residues [72]. Then, in all cases, there could be a combination of physical adsorption and chemisorption. Furthermore, the calculated and tabulated values of q_e in Table 4 are close to the experimental values. Riahi et al. [73] reported that the pseudo-second-order model fits throughout the evaluated adsorption period and supports the assumption that adsorption is due to chemisorption through ion exchange until the vacant sites are occupied, then molecules diffuse into the adsorbent pores.
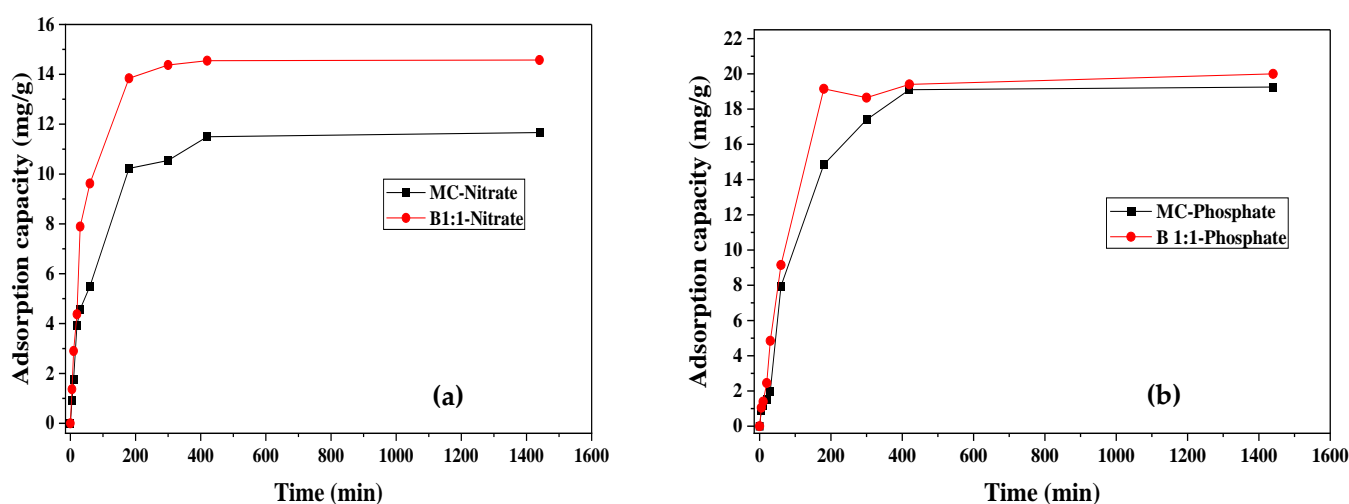

Figure 7. Adsorption kinetics for (**a**) nitrate and (**b**) phosphate.

The pseudo-second-order model also described the kinetics of phosphate on two stable organometallic structures functionalized with amino groups; the mechanism controlling adsorption was inferred as chemical removal implicating valence forces by giving electrons between bio-adsorbent and adsorbate, according to the selectivity [65]. Similar results were obtained using ion exchange resins prepared from corn and yucca husks quaternized with epichlorohydrin, *N,N*-dimethylformamide, and pyridine; maximum removal capacities of 53.1 and 82.18 were obtained when an initial concentration of 200 mg/L was used [59]. When using corn stalks modified with triethylenetetramine and triethyleneamine, q_e of 15.71 and 20.48 mg/g of nitrate and phosphate, respectively, was obtained; it was also found that the dates were described by a pseudo-second-order model [48]. The general explanation for the mechanism of kinetic law involves a variation of the energetics of chemisorption with the active sites that are heterogeneous on bio-adsorbents and also show different activation energies for reactions because their cell walls primarily consist of cellulose, and many hydroxyl groups, such as tannins or other phenolic compounds [73]. Thereby, it may depict the breakthrough curve in a packed bed column; a global mass balance could do this to get equations for the breakthrough curve in a bed packed with adsorbent. Then, the obtained equations can be employed for scaling up and designing the adsorption beds for a liquid-solid system, considering that real adsorption systems operate continuously to treat large volumes of polluted water [74].

3.5. Multi-Component Adsorption

Competitive contaminant removal studies provide insight into the practical application of adsorption since superior adsorbents must possess fast adsorption kinetics, high removal capacity, and specific selectivity towards specific contaminants; This, considering that in real wastewater, a mixture of various ions coexists and compete for adsorption sites [65]. Therefore, it is interesting to test the selectivity of adsorbents by employing competitive adsorption tests.

Figure 8 shows the competitive removal of nitrate and phosphate, showing an increase in selectivity by both bio-adsorbents for the phosphate anion, which can be attributed to the trivalent nature of the anion, potentially giving it higher selectivity. The use of MC increased the percentage of phosphate removal compared to the selective experiments, while the behavior of the nitrate anion remained with similar efficiencies. On the other hand, when using B 1:1 sample, it was found that nitrate removal efficiency decreased while phosphate removal increased. This fact can be explained, according to Helfferich's concept of electros-selectivity, adsorbents tend to prefer higher valence counterions to lower valence ones [75]. Considering that the working pH was 4 and the dominant phosphorus species were $HPO_4^{2-}/H_2PO_4^{-}$, nitrate did not strongly affect phosphate adsorption. In addition to the ionic interaction, ligand exchange through forming a chemical bond between phosphate and the quaternary nitrogen species also contributed to the adsorption process, which ensured high performance in a simple system towards phosphate [65]. Nitrate presented the lowest removal, possibly due to its monovalent nature; it would have a higher selectivity for specific bio-adsorbent active centers [76]. This fact may be due to the anionic charges of multivalent PO_4^{3-} ions which have a higher density and are adsorbed faster than monovalent ions [77]. Likewise, it could be due to the ease of phosphate ions to transfer from the liquid to the solid phase, at a constant temperature and pressure, towards nitrate during adsorption. Thus, it coincides with the reported use of hybrid chitosan beads grafted with the amine [78].
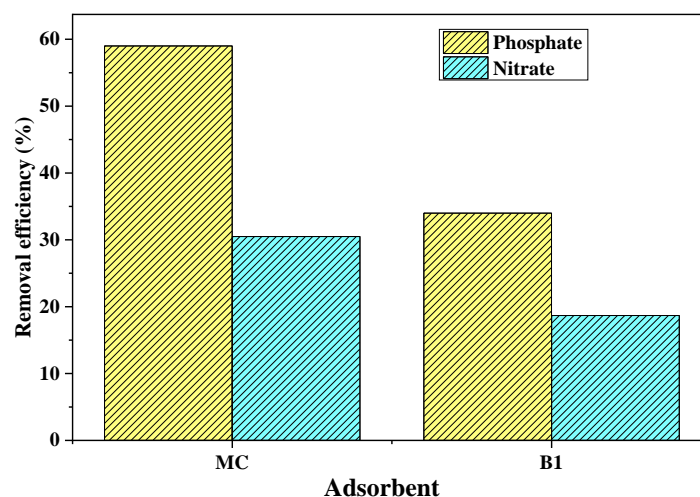

Figure 8. Competitive removal of Nitrate and Phosphate.

Similar findings were obtained when evaluating the coexistence of different anions on phosphate removal. Their interference was negligible because phosphate ions bind more to the surface of the adsorbents due to their multivalent nature [1]. Also, when using dolomite, it was found that nitrate does not alter the phosphate adsorption capacity [3]. In addition, Jeyaseelan and Viswanathan [79] reported during the competitive fluoride adsorption in the presence of chlorine, phosphate, sulfate, nitrate, and bicarbonate. The increasing removal efficiency of NO_3^{-} in the presence of PO_4^{3-} might be because phosphate in an aqueous solution produces hydroxyl ions, which raises the pH of the solution. These probably elevated deprotonation to such an extent that the MC's surface may become electronegative, altering the electrostatic for their attraction into electrostatic repulsion,

which causes the adverse effect. This would explain the higher efficiency of the two adsorbents regarding the selective tests (Figure 4).

4. Conclusions

From the adsorption essays and characterization of the bio-adsorbents, this study concluded that the agricultural residues in corn stalks are copious residues that can be used for extracting cellulose. The chemical modification of this cellulose with the CTAC compound allowed protonating of the biomass surface, making this bio-adsorbent attractive for removing nitrate and phosphate anions in a batch system. Moreover, biochar was successfully prepared by the impregnation methodology using H_2SO_4. SEM-EDS analysis showed that the bio-adsorbent B 1:1 exhibited a heterogeneous surface of porous nature with macro and mesopores with agglutinated networks. At the same time, the MC sample had a slightly porous surface with the presence of multiple folds. In addition, the effect of temperature was evaluated, finding that the best efficiencies of nitrate removal on MC and phosphate removal on B 1:1 occurred at 30 °C, phosphate removal on MC at 35 °C, and nitrate removal on B 1:1 occurred at 25 °C. The equilibrium was reached at 420 min, achieving the highest adsorption capacity of nitrate and phosphate over B 1:1. Nitrate adsorption with MC showed a good fit to the pseudo-second-order model. The pseudo-first-order model described the kinetics of phosphate removal with MC bio-adsorbent and both anions (nitrate and phosphate) over B 1:1 bio-adsorbent. Freundlich's model fits the nitrate and phosphate experimental data with an acceptable level of accuracy, indicating that the process is multi-layered. The multi-component study evidences the selectivity of biomaterials by phosphate without indicating competition for the material's active centers among the anions studied, suggesting the potential applications of the carbon-based bio-adsorbents for anionic ions remotion in aqueous media.

References

1. Alagha, O.; Manzar, M.S.; Zubair, M.; Anil, I.; Mu'azu, N.D.; Qureshi, A. Comparative adsorptive removal of phosphate and nitrate from wastewater using biochar-MgAl LDH nanocomposites: Coexisting anions effect and mechanistic studies. *Nanomaterials* **2020**, *10*, 336. [CrossRef]
2. Rashidi Nodeh, H.; Sereshti, H.; Zamiri Afsharian, E.; Nouri, N. Enhanced removal of phosphate and nitrate ions from aqueous media using nanosized lanthanum hydrous doped on magnetic graphene nanocomposite. *J. Environ. Manag.* **2017**, *197*, 265–274. [CrossRef] [PubMed]
3. Boeykens, S.P.; Piol, M.N.; Samudio Legal, L.; Saralegui, A.B.; Vázquez, C. Eutrophication decrease: Phosphate adsorption processes in presence of nitrates. *J. Environ. Manag.* **2017**, *203*, 888–895. [CrossRef]
4. Pu, J.; Wang, S.; Ni, Z.; Wu, Y.; Liu, X.; Wu, T.; Wu, H. Implications of phosphorus partitioning at the suspended particle-water interface for lake eutrophication in China's largest freshwater lake, Poyang Lake. *Chemosphere* **2021**, *263*, 128334. [CrossRef]
5. Singh, S.; Anil, A.G.; Kumar, V.; Kapoor, D.; Subramanian, S.; Singh, J.; Ramamurthy, P.C. Nitrates in the environment: A critical review of their distribution, sensing techniques, ecological effects and remediation. *Chemosphere* **2022**, *287*, 131996. [CrossRef] [PubMed]

6. Mahmud, M.A.P.; Ejeian, F.; Azadi, S.; Myers, M.; Pejcic, B.; Abbassi, R.; Razmjou, A.; Asadnia, M. Recent progress in sensing nitrate, nitrite, phosphate, and ammonium in aquatic environment. *Chemosphere* **2020**, *259*, 127492. [CrossRef]

7. Mukimin, A.; Vistanty, H.; Zen, N.; Purwanto, A.; Wicaksono, K.A. Performance of bioequalization-electrocatalytic integrated method for pollutants removal of hand-drawn batik wastewater. *J. Water Process Eng.* **2018**, *21*, 77–83. [CrossRef]

8. Zhao, T.; Feng, T. Application of modified chitosan microspheres for nitrate and phosphate adsorption from aqueous solution. *RSC Adv.* **2016**, *6*, 90878–90886. [CrossRef]

9. Hassan, W.; Farooq, U.; Ahmad, M.; Athar, M.; Khan, M. Potential biosorbent, Haloxylon recurvum plant stems, for the removal of methylene blue dye. *Arab. J. Chem.* **2017**, *10*, 1512–1522. [CrossRef]

10. Yin, Q.; Zhang, B.; Wang, R.; Zhao, Z. Biochar as an adsorbent for inorganic nitrogen and phosphorus removal from water: A review. *Environ. Sci. Pollut. Res.* **2017**, *24*, 26297–26309. [CrossRef]

11. Almanassra, I.W.; Mckay, G.; Kochkodan, V.; Ali Atieh, M.; Al-Ansari, T. A state of the art review on phosphate removal from water by biochars. *Chem. Eng. J.* **2021**, *409*, 128211. [CrossRef]

12. Ahamad, T.; Naushad, M.; Ubaidullah, M.; Alshehri, S. Fabrication of highly porous polymeric nanocomposite for the removal of radioactive U(VI) and Eu(III) ions from aqueous solution. *Polymers* **2020**, *12*, 2940. [CrossRef] [PubMed]

13. Öztürk, N.; Bektaş, T.E. Nitrate removal from aqueous solution by adsorption onto various materials. *J. Hazard Mater.* **2004**, *112*, 155–162. [CrossRef] [PubMed]

14. Golie, W.M.; Upadhyayula, S. An investigation on biosorption of nitrate from water by chitosan based organic-inorganic hybrid biocomposites. *Int. J. Biol. Macromol.* **2017**, *97*, 489–502. [CrossRef]

15. Prashantha Kumar, T.K.M.; Mandlimath, T.R.; Sangeetha, P.; Revathi, S.K.; Ashok Kumar, S.K. Nanoscale materials as sorbents for nitrate and phosphate removal from water. *Environ. Chem. Lett.* **2018**, *16*, 389–400. [CrossRef]

16. Yin, Q.; Wang, R.; Zhao, Z. Application of Mg–Al-modified biochar for simultaneous removal of ammonium, nitrate, and phosphate from eutrophic water. *J. Clean. Prod.* **2018**, *176*, 230–240. [CrossRef]

17. Manjunath, S.V.; Kumar, M. Evaluation of single-component and multi-component adsorption of metronidazole, phosphate and nitrate on activated carbon from *Prosopis juliflora*. *Chem. Eng. J.* **2018**, *346*, 525–534. [CrossRef]

18. Hao, P.; Shi, Y.; Li, S.; Zhu, X.; Cai, N. Correlations between adsorbent characteristics and the performance of pressure swing adsorption separation process. *Fuel* **2018**, *230*, 9–17. [CrossRef]

19. Naushad, M.; Sharma, G.; Kumar, A.; Sharma, S.; Ghfar, A.A.; Bhatnagar, A.; Stadler, F.J.; Khan, M.R. Efficient removal of toxic phosphate anions from aqueous environment using pectin based quaternary amino anion exchanger. *Int. J. Biol. Macromol.* **2018**, *2018*, 1–10. [CrossRef]

20. Xi, Y.; Huang, M.; Luo, X. Enhanced phosphate adsorption performance by innovative anion imprinted polymers with dual interaction. *Appl. Surf. Sci.* **2019**, *467*, 135–142. [CrossRef]

21. Huong, P.T.; Jitae, K.; Giang, B.L.; Nguyen, T.D.; Thang, P.Q. Novel lanthanum-modified activated carbon derived from pine cone biomass as ecofriendly bio-sorbent for removal of phosphate and nitrate in wastewater. *Rend. Lincei* **2019**, *30*, 637–647. [CrossRef]

22. Konneh, M.; Wandera, S.M.; Murunga, S.I.; Raude, J.M. Adsorption and desorption of nutrients from abattoir wastewater: Modelling and comparison of rice, coconut and coffee husk biochar. *Heliyon* **2021**, *7*, e08458. [CrossRef] [PubMed]

23. Stjepanović, M.; Velić, N.; Lončarić, A.; Gašo-Sokač, D.; Bušić, V.; Habuda-Stanić, M. Adsorptive removal of nitrate from wastewater using modified lignocellulosic waste material. *J. Mol. Liq.* **2019**, *285*, 535–544. [CrossRef]

24. Manyatshe, A.; Cele, Z.E.D.; Balogun, M.O.; Nkambule, T.T.I.; Msagati, T.A.M. Chitosan modified sugarcane bagasse biochar for the adsorption of inorganic phosphate ions from aqueous solution. *J. Environ. Chem. Eng.* **2022**, *10*, 108243. [CrossRef]

25. Namasivayam, C.; Höll, W.H. Quaternized biomass as an anion exchanger for the removal of nitrate and other anions from water. *J. Chem. Technol. Biotechnol.* **2005**, *80*, 164–168. [CrossRef]

26. Dong, S.; Ji, Q.; Wang, Y.; Liu, H.; Qu, J. Enhanced phosphate removal using zirconium hydroxide encapsulated in quaternized cellulose. *J. Environ. Sci.* **2020**, *89*, 102–122. [CrossRef]

27. Du, J.; Dong, Z.; Yang, X.; Zhao, L. Radiation grafting of dimethylaminoethyl methacrylate on cotton linter and subsequent quaternization as new eco-friendly adsorbent for phosphate removal. *Environ. Sci. Pollut. Res.* **2020**, *27*, 24558–24567. [CrossRef]

28. Wang, H.; Wang, S.; Gao, Y. Cetyl trimethyl ammonium bromide modified magnetic biochar from pine nut shells for efficient removal of acid chrome blue K. *Bioresour. Technol.* **2020**, *312*, 123564. [CrossRef]

29. Al-Jubory, F.K.; Mujtaba, I.M.; Abbas, A.S. Preparation and characterization of biodegradable crosslinked starch ester as adsorbent. *AIP Conf. Proc.* **2020**, *2213*, 020165. [CrossRef]

30. Zhang, Y.; Li, Y.; Song, Y.; Li, J. Synthesis and aggregation behaviors of tail-branched surfactant Guerbet-cetyl trimethyl ammonium chloride. *Colloid Polym. Sci.* **2015**, *294*, 271–279. [CrossRef]

31. Delgado Villafuerte, C.R.; Hidalgo Zambrano, K.M.; Villafuerte Vélez, C.A.; Noles Aguilar, P.J.; Richard, E. Effect on the resistance blocks elaborated with corn cultivates wastes (*Zea mays*). *Rev. Iberoam. Ambient. Sustentabilidad* **2019**, *2*, 89–98. [CrossRef]

32. Correa, H.J. Yield and nutritional quality of maize stalk syrup in Colombia. *Livest. Res. Rural Dev.* **2013**, *25*, 25–28.

33. Xu, J.; Krietemeyer, E.F.; Boddu, V.M.; Liu, S.X.; Liu, W.C. Production and characterization of cellulose nanofibril (CNF) from agricultural waste corn stover. *Carbohydr. Polym.* **2018**, *192*, 202–207. [CrossRef] [PubMed]

34. Xia, F.; Yang, H.; Li, L.; Ren, Y.; Shi, D.; Chai, H.; Ai, H.; He, Q.; Gu, L. Enhanced nitrate adsorption by using cetyltrimethylammonium chloride pre-loaded activated carbon. *Environ. Technol.* **2019**, 3562–3572. [CrossRef]

35. Herrera-Barros, A.; Tejada-Tovar, C.; Villabona-Ortíz, A.; Gonzalez-Delgado, A.D.; Benitez-Monroy, J. Cd (II) and Ni (II) uptake by novel biosorbent prepared from oil palm residual biomass and Al2O3 nanoparticles. *Sustain. Chem. Pharm.* **2020**, *15*, 100216. [CrossRef]

36. *ASTM D 515-60*; Standard Test Method for Phosphate Ion in Water. ASTM: West Conshohocken, PA, USA, 2018; pp. 1–4.

37. *ASTM D7781—14*; Standard Test Method for Nitrite-Nitrate in Water by Nitrate Reductase. ASTM: West Conshohocken, PA, USA, 2018; pp. 1–8.

38. Rasmey, A.-H.M.; Aboseidah, A.A.; Youssef, A.K. Application of Langmuir and Freundlich Isotherm Models on Biosorption of Pb2+ by Freez-dried Biomass of Pseudomonas aeruginosa. *Egypt. J. Microbiol.* **2018**, *53*, 37–48. [CrossRef]

39. Banchhor, A.; Pandey, M.; Pandey, P.K. Optimization of Adsorption Parameters for Effective Removal of Hexavalent Chromium Using Simarouba glauca from Aqueous Solution. *Water Conserv. Sci. Eng.* **2021**, *6*, 127–144. [CrossRef]

40. Mohsenibandpei, A.; Ghaderpoori, M.; Hassani, G.; Bahrami, H.; Bahmani, Z.; Alinejad, A.A. Water solution polishing of nitrate using potassium permanganate modified zeolite: Parametric experiments, kinetics and equilibrium analysis. *Glob. Nest J.* **2016**, *18*, 546–558. [CrossRef]

41. Lonappan, L.; Rouissi, T.; Brar, S.K.; Verma, M.; Surampalli, R.Y. An insight into the adsorption of diclofenac on different biochars: Mechanisms, surface chemistry, and thermodynamics. *Bioresour. Technol.* **2018**, *249*, 386–394. [CrossRef]

42. Hubbe, M.A.; Azizian, S.; Douven, S. Implications of apparent pseudo-second-order adsorption kinetics onto cellulosic materials: A review. *BioResources* **2019**, *14*, 7582–7626. [CrossRef]

43. Lemita, N.; Deghboudj, S.; Rokbi, M.; Rekbi, F.M.L.; Halimi, R. Characterization and analysis of novel natural cellulosic fiber extracted from Strelitzia reginae plant. *J. Compos. Mater.* **2021**, *56*, 99–114. [CrossRef]

44. Rasheed, M.; Jawaid, M.; Parveez, B.; Zuriyati, A.; Khan, A. Morphological, chemical and thermal analysis of cellulose nanocrystals extracted from bamboo fibre. *Int. J. Biol. Macromol.* **2020**, *160*, 183–191. [CrossRef] [PubMed]

45. Katakojwala, R.; Mohan, S.V. Microcrystalline cellulose production from sugarcane bagasse: Sustainable process development and life cycle assessment. *J. Clean. Prod.* **2020**, *249*, 119342. [CrossRef]

46. Fan, C.; Zhang, Y. Adsorption isotherms, kinetics and thermodynamics of nitrate and phosphate in binary systems on a novel adsorbent derived from corn stalks. *J. Geochemical. Explor.* **2018**, *188*, 95–100. [CrossRef]

47. Mohebali, S.; Bastani, D.; Shayesteh, H. Equilibrium, kinetic and thermodynamic studies of a low-cost biosorbent for the removal of Congo red dye: Acid and CTAB-acid modified celery (*Apium graveolens*). *J. Mol. Struct.* **2019**, *1176*, 181–193. [CrossRef]

48. Wang, L.; Xu, Z.; Fu, Y.; Chen, Y.; Pan, Z.; Wang, R.; Tan, Z. Comparative analysis on adsorption properties and mechanisms of nitrate and phosphate by modified corn stalks. *RSC Adv.* **2018**, *8*, 36468–36476. [CrossRef]

49. Hastati, D.Y.; Hambali, E.; Syamsu, K.; Warsiki, E. Enhanced Hydrophobicity of Nanofibrillated Cellulose Through Surface Modification Using Cetyltrimethylammonium Chloride Derived from Palmityl Alcohol. *Waste Biomass Valorization* **2021**, *12*, 5147–5159. [CrossRef]

50. Ren, Z.; Xu, X.; Wang, X.; Gao, B.; Yue, Q.; Song, W.; Zhang, L.; Wang, H. FTIR, Raman, and XPS analysis during phosphate, nitrate and Cr(VI) removal by amine cross-linking biosorbent. *J. Colloid Interface Sci.* **2016**, *468*, 313–323. [CrossRef]

51. Qiao, H.; Mei, L.; Chen, G.; Liu, H.; Peng, C.; Ke, F.; Hou, R.; Wan, X.; Cai, H. Adsorption of nitrate and phosphate from aqueous solution using amine cross-linked tea wastes. *Appl. Surf. Sci.* **2019**, *483*, 114–122. [CrossRef]

52. Kumar, A.; Negi, Y.S.; Choudhary, V.; Bhardwaj, N.K. Characterization of Cellulose Nanocrystals Produced by Acid-Hydrolysis from Sugarcane Bagasse as Agro-Waste. *J. Mater. Phys. Chem.* **2014**, *2*, 1–8. [CrossRef]

53. Eleryan, A.; El Nemr, A.; Idris, A.M.; Alghamdi, M.M.; El-Zahhar, A.A.; Said, T.O.; Sahlabji, T. Feasible and eco-friendly removal of hexavalent chromium toxicant from aqueous solutions using chemically modified sugarcane bagasse cellulose. *Toxin Rev.* **2020**, *40*, 1–12. [CrossRef]

54. Pap, S.; Bezanovic, V.; Radonic, J.; Babic, A.; Saric, S.; Adamovic, D.; Turk Sekulic, M. Synthesis of highly-efficient functionalized biochars from fruit industry waste biomass for the removal of chromium and lead. *J. Mol. Liq.* **2018**, *268*, 315–325. [CrossRef]

55. Peiris, C.; Nayanathara, O.; Navarathna, C.M.; Jayawardhana, Y.; Nawalage, S.; Burk, G.; Karunanayake, A.G.; Madduri, S.B.; Vithanage, M.; Kaumal, M.N.; et al. The influence of three acid modifications on the physicochemical characteristics of tea-waste biochar pyrolyzed at different temperatures: A comparative study. *RSC Adv.* **2019**, *9*, 17612–17622. [CrossRef] [PubMed]

56. Yin, Q.; Ren, H.; Wang, R.; Zhao, Z. Evaluation of nitrate and phosphate adsorption on Al-modified biochar: Influence of Al content. *Sci. Total Environ.* **2018**, *631*, 895–903. [CrossRef] [PubMed]

57. Angulo-Padilla, J.; Lozano-De, L.; Ossa, L.; González-Delgado, Á.; Sánchez-Tuirán, E.; Ojeda-Delgado, K. Potential for Degradation of Lignocellulosic Biomass via Alkaline Pretreatment Using Corn Crop Residual Biomass. *Contemp. Eng. Sci.* **2018**, *11*, 679–687. [CrossRef]

58. Liu, Y.; Xie, J.; Wu, N.; Ma, Y.; Menon, C.; Tong, J. Characterization of natural cellulose fiber from corn stalk waste subjected to different surface treatments. *Cellulose* **2019**, *26*, 4707–4719. [CrossRef]

59. Banu, H.A.T.; Karthikeyan, P.; Meenakshi, S. Comparative studies on revival of nitrate and phosphate ions using quaternized corn husk and jackfruit peel. *Bioresour. Technol. Rep.* **2019**, *8*, 100331. [CrossRef]

60. Ranasinghe, S.H.; Navaratne, A.N.; Priyantha, N. Enhancement of adsorption characteristics of Cr(III) and Ni(II) by surface modification of jackfruit peel biosorbent. *J. Environ. Chem. Eng.* **2018**, *6*, 5670–5682. [CrossRef]

61. Udoetok, I.A.; Dimmick, R.M.; Wilson, L.D.; Headley, J.V. Adsorption properties of cross-linked cellulose-epichlorohydrin polymers in aqueous solution. *Carbohydr. Polym.* **2016**, *136*, 329–340. [CrossRef]

62. Zimmermann, R.; Freudenberg, U.; Schweiß, R.; Küttner, D.; Werner, C. Hydroxide and hydronium ion adsorption—A survey. *Curr. Opin. Colloid Interface Sci.* **2010**, *15*, 196–202. [CrossRef]

63. Halajnia, A.; Oustan, S.; Najafi, N.; Khataee, A.R.; Lakzian, A. Adsorption-desorption characteristics of nitrate, phosphate and sulfate on Mg-Al layered double hydroxide. *Appl. Clay Sci.* **2013**, *80*, 305–312. [CrossRef]

64. Banu, H.T.; Meenakshi, S.; Elsevier, B.V. *One Pot Synthesis of Chitosan Grafted Quaternized Resin for the Removal of Nitrate and Phosphate from Aqueous Solution*; Elsevier B.V.: Amsterdam, The Netherlands, 2017; Volume 104, ISBN 9145124523.

65. Liu, R.; Chi, L.; Wang, X.; Wang, Y.; Sui, Y.; Xie, T.; Arandiyan, H. Effective and selective adsorption of phosphate from aqueous solution via trivalent-metals-based amino-MIL-101 MOFs. *Chem. Eng. J.* **2019**, *357*, 159–168. [CrossRef]

66. Abdolali, A.; Ngo, H.H.; Guo, W.; Zhou, J.L.; Zhang, J.; Liang, S.; Chang, S.W.; Nguyen, D.D.; Liu, Y. Application of a breakthrough biosorbent for removing heavy metals from synthetic and real wastewaters in a lab-scale continuous fixed-bed column. *Bioresour. Technol.* **2017**, *229*, 78–87. [CrossRef] [PubMed]

67. Barroso-Solares, S.; Merillas, B.; Cimavilla-Román, P.; Rodriguez-Perez, M.A.; Pinto, J. Enhanced nitrates-polluted water remediation by polyurethane/sepiolite cellular nanocomposites. *J. Clean. Prod.* **2020**, *254*, 120038. [CrossRef]

68. Karthikeyan, P.; Meenakshi, S. Synthesis and characterization of Zn–Al LDHs/activated carbon composite and its adsorption properties for phosphate and nitrate ions in aqueous medium. *J. Mol. Liq.* **2019**, *296*, 111766. [CrossRef]

69. Matusik, J. Arsenate, orthophosphate, sulfate, and nitrate sorption equilibria and kinetics for halloysite and kaolinites with an induced positive charge. *Chem. Eng. J.* **2014**, *246*, 244–253. [CrossRef]

70. Ganguly, P.B.; Krishnamurti, S. An application of the Donnan theory to the adsorption of ions by colloidal silicic acid. *Trans. Faraday Soc.* **1928**, *24*, 401–405. [CrossRef]

71. Guaya, D.; Valderrama, C.; Farran, A.; Armijos, C.; Cortina, J.L. Simultaneous phosphate and ammonium removal from aqueous solution by a hydrated aluminum oxide modified natural zeolite. *Chem. Eng. J.* **2015**, *271*, 204–213. [CrossRef]

72. Wang, H.; Shen, H.; Shen, C.; Li, Y.; Ying, Z.; Duan, Y. Kinetics and Mechanism Study of Mercury Adsorption by Activated Carbon in Wet Oxy-Fuel Conditions. *Energy Fuels* **2019**, *33*, 1344–1353. [CrossRef]

73. Riahi, K.; Chaabane, S.; Thayer, B. Ben A kinetic modeling study of phosphate adsorption onto *Phoenix dactylifera* L. date palm fibers in batch mode. *J. Saudi Chem. Soc.* **2017**, *21*, S143–S152. [CrossRef]

74. Das, G.K.; Chatterjee, S. Use of Kinetic Models for Correlating Adsorbate Breakthrough in a Fixed Bed of Adsorbent. In Proceedings of the CHEMCON 2007, Kolkata, India, 27–30 December 2007.

75. Loganathan, P.; Vigneswaran, S.; Kandasamy, J.; Bolan, N.S. Removal and Recovery of Phosphate from Water Using Sorption. *Crit. Rev. Environ. Sci. Technol.* **2014**, *44*, 847–907. [CrossRef]

76. Iftekhar, S.; Küçük, M.E.; Srivastava, V.; Repo, E.; Sillanpää, M. Application of zinc-aluminium layered double hydroxides for adsorptive removal of phosphate and sulfate: Equilibrium, kinetic and thermodynamic. *Chemosphere* **2018**, *209*, 470–479. [CrossRef] [PubMed]

77. Aswin Kumar, I.; Viswanathan, N. Development and Reuse of Amine-Grafted Chitosan Hybrid Beads in the Retention of Nitrate and Phosphate. *J. Chem. Eng. Data* **2018**, *63*, 147–158. [CrossRef]

78. Song, W.; Gao, B.; Xu, X.; Wang, F.; Xue, N.; Sun, S.; Song, W.; Jia, R. Adsorption of nitrate from aqueous solution by magnetic amine-crosslinked biopolymer based corn stalk and its chemical regeneration property. *J. Hazard. Mater.* **2016**, *304*, 280–290. [CrossRef]

79. Jeyaseelan, A.; Viswanathan, N. Investigation of Hydroxyapatite-Entrenched Cerium Organic Frameworks Incorporating Biopolymeric Beads for Efficient Fluoride Removal. *Ind. Eng. Chem. Res.* **2022**, *61*, 7911–7925. [CrossRef]